



## Reproducibility of ZrO<sub>2</sub>-based freeze casting for biomaterials



Steven E. Naleway<sup>a,\*</sup>, Kate C. Fickas<sup>b</sup>, Yajur N. Maker<sup>c</sup>, Marc A. Meyers<sup>a,d,e</sup>, Joanna McKittrick<sup>a,d</sup>

<sup>a</sup> Materials Science and Engineering Program, University of California, San Diego, 9500 Gilman Drive, La Jolla, CA 92093, USA

<sup>b</sup> Department of Forest Ecosystems and Society, Oregon State University, 321 Richardson Hall, Corvallis, OR 97331, USA

<sup>c</sup> Department of Bioengineering, University of California, San Diego, 9500 Gilman Drive, La Jolla, CA 92093, USA

<sup>d</sup> Department of Mechanical and Aerospace Engineering, University of California, San Diego, 9500 Gilman Drive, La Jolla, CA 92093, USA

<sup>e</sup> Department of NanoEngineering, University of California, San Diego, 9500 Gilman Drive, La Jolla, CA 92093, USA

### ARTICLE INFO

#### Article history:

Received 7 July 2015

Received in revised form 4 November 2015

Accepted 7 December 2015

Available online 11 December 2015

#### Keywords:

Freeze casting

Bioinspired

Biomaterial

Statistical analysis

Reproducibility

Mechanical properties

### ABSTRACT

The processing technique of freeze casting has been intensely researched for its potential to create porous scaffold and infiltrated composite materials for biomedical implants and structural materials. However, in order for this technique to be employed medically or commercially, it must be able to reliably produce materials in great quantities with similar microstructures and properties. Here we investigate the reproducibility of the freeze casting process by independently fabricating three sets of eight ZrO<sub>2</sub>-epoxy composite scaffolds with the same processing conditions but varying solid loading (10, 15 and 20 vol.%). Statistical analyses (One-way ANOVA and Tukey's HSD tests) run upon measurements of the microstructural dimensions of these composite scaffold sets show that, while the majority of microstructures are similar, in all cases the composite scaffolds display statistically significant variability. In addition, composite scaffolds where mechanically compressed and statistically analyzed. Similar to the microstructures, almost all of their resultant properties displayed significant variability though most composite scaffolds were similar. These results suggest that additional research to improve control of the freeze casting technique is required before scaffolds and composite scaffolds can reliably be reproduced for commercial or medical applications.

© 2015 Elsevier B.V. All rights reserved.

### 1. Introduction

The freeze casting process has been greatly researched over the past decade as an attractive method to fabricate bioinspired materials and composites [1–9]. The process itself is carried out in four steps: (1) a slurry of solid loading (e.g. ceramic particles) and a liquid freezing agent (e.g. water) is prepared, (2) the slurry is directionally frozen in a controlled manner, causing the liquid freezing agent to template the solid loading, (3) the frozen scaffold is freeze dried in order to remove the freezing agent and create a green body, and (4) the green body is sintered in order to form a final, porous scaffold where the ice crystals have been converted into aligned pores [1,3,4,8]. Once these porous scaffolds have been fabricated, they can be infiltrated with polymers or metals in order to create two-phase interpenetrating composites [5,10–12].

Given that the constituents and mechanical properties can be tailored, a common prospective application for these scaffolds and composites is mimetic bone [13–16]. While this application shows great promise, any biomedical implant material will need to undergo rigorous

certification and testing. Additionally, any commercial applications will require that numerous samples be made that are effectively, if not entirely, the same. In both cases, samples will need to be reproducibly created with similar mechanical and geometric properties. However, to the knowledge of the authors there has yet to be any statistical study on the reproducibility of this freeze casting method.

In this we investigate the reproducibility of freeze cast composite materials for bioinspired and biomimetic applications. This is done by focusing upon three sets of ZrO<sub>2</sub>-epoxy freeze cast composite scaffolds, which were frozen with water as a freezing agent and varied in solid loading concentration. While other base constituents or variations on the freeze casting process may produce differing results, we propose this work as a reference point for not only academic research, but also potential commercial applications.

### 2. Materials and methods

#### 2.1. Sample preparation

Aqueous slurries were prepared in order to investigate the reproducibility of the freeze casting process. To create three individual sample sets with varying solid loading, slurries consisting of 10, 15 and 20 vol.% ZrO<sub>2</sub> powders (200–500 nm diameter) (Sigma Aldrich, St. Louis, MO, USA) were mixed with 1 wt.% polyvinyl alcohol (PVA) with

\* Corresponding author.

E-mail addresses: [snaleway@eng.ucsd.edu](mailto:snaleway@eng.ucsd.edu) (S.E. Naleway), [kate.fickas@oregonstate.edu](mailto:kate.fickas@oregonstate.edu) (K.C. Fickas), [ymaker@eng.ucsd.edu](mailto:ymaker@eng.ucsd.edu) (Y.N. Maker), [mameyers@eng.ucsd.edu](mailto:mameyers@eng.ucsd.edu) (M.A. Meyers), [jmckittrick@eng.ucsd.edu](mailto:jmckittrick@eng.ucsd.edu) (J. McKittrick).

a molecular weight of 100,000 g/mol (Alfa Aesar, Ward Hill, MA, USA) as a binder, 1 wt.% polyethylene glycol (PEG) with a molecular weight of 10,000 g/mol (Alfa Aesar, Ward Hill, MA, USA) as a binder and 1 wt.% of an anionic dispersant, Darvan 811 (R. T. Vanderbilt Company, Inc., Norwalk, CT, USA) to ensure a homogeneous slurry. Slurries were created for each individual scaffold. For each solid loading concentration (10, 15 and 20 vol.% ZrO<sub>2</sub>), eight identical solutions (water, PVA, PEG and dispersant) were created with a volume of 16 mL. All slurries

were ball milled in an alumina grinding medium for ~24 h then degassed under low vacuum for 5–15 min. From each slurry, samples of approximately 8–10 mL of the degassed slurry were poured into a freeze cast mold and frozen at a constant rate of 10 K/min using a custom built freeze casting device, as previously described [7]. Subsequent to freezing, samples were lyophilized in a bench-top freeze dryer (Labconco, Kansas City, MO, USA) at 223 K and 350 Pa for 70 h so as to sublime out the frozen water. After freeze drying, the green bodies

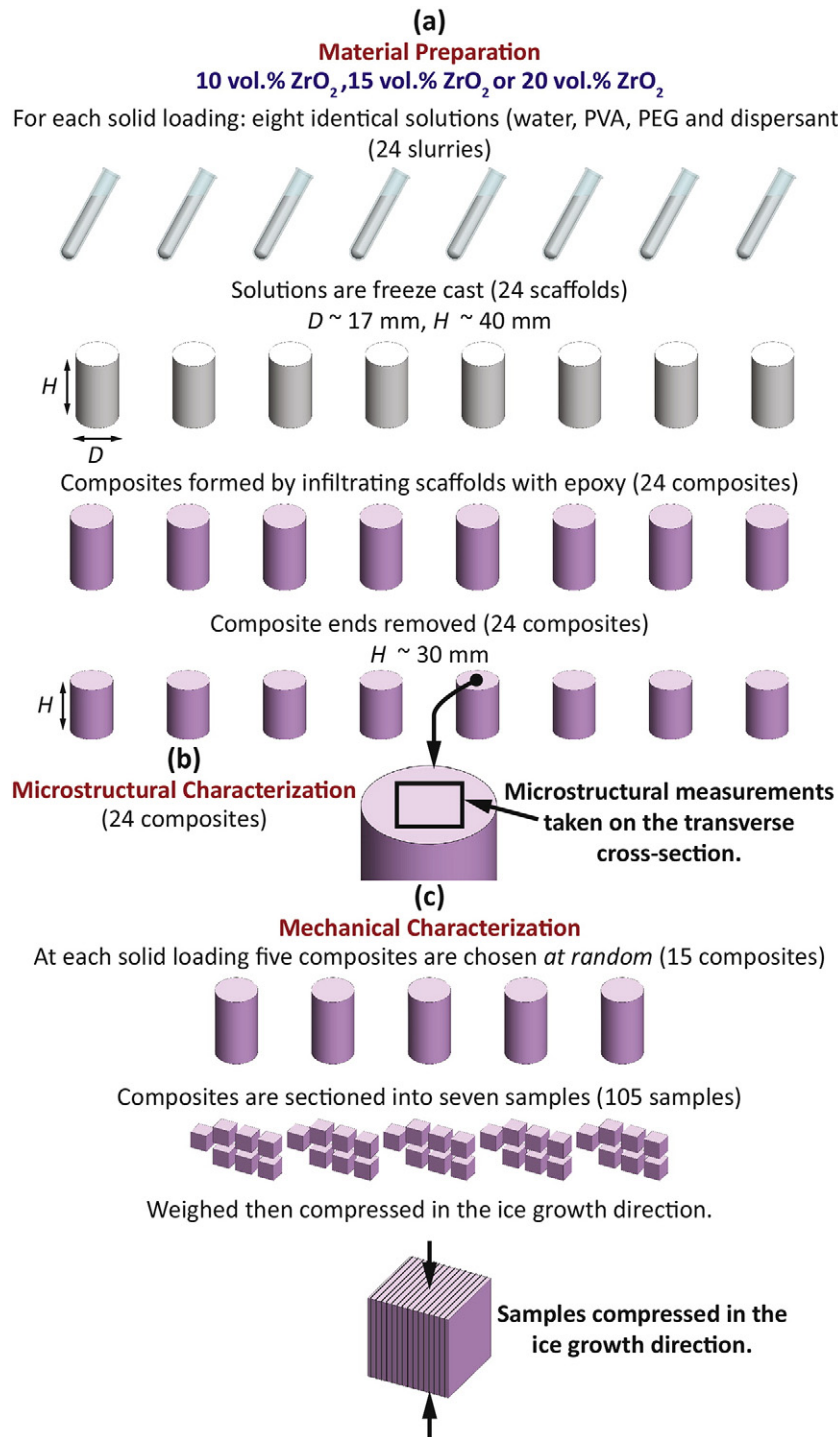


**Fig. 1.** Schematic of the fabricated samples and performed tests for each solid loading (10, 15 and 20 vol.% ZrO<sub>2</sub>). (a) For each solid loading, eight identical solutions (water, PVA, PEG and dispersant) were created and freeze cast to form scaffolds with diameters and heights of ~17 and 40 mm respectively. Each scaffold was infiltrated with epoxy to form a composite and had the ends removed to result in a final height of ~30 mm; (b) microstructural characterization was performed by taking measurements from SEM analysis on the transverse cross-sections of each composite; (c) to perform mechanical characterization, at each solid loading five composites were selected *at random* and sectioned into seven samples, each  $5 \times 5 \times 5$  mm<sup>3</sup>. These samples were weighed and compressed in the ice growth direction.

were sintered in an open air furnace for 3 h at 1623 K with heating and cooling rates of 2 K/min. This sintering procedure is similar to processes reported as effective for ZrO<sub>2</sub> scaffolds [6,7]. A total of eight scaffolds were prepared for each solid loading concentration (10, 15 and 20 vol.% ZrO<sub>2</sub>) for a total of 24 scaffolds. For clarity, the samples created and tests (as described in the subsequent sections) are schematically visualized in Fig. 1.

Each scaffold in the three sets was infiltrated with an epoxy, Epocure 2 (Buehler, Lake Bluff, IL, USA) by in situ polymerization in order to form a ceramic–polymer composite for imaging and mechanical testing. Samples were immersed in a mixture of liquid monomer and catalyst under low vacuum for 20–30 min in order to force the liquid to infiltrate the scaffold pores. The infiltrated scaffolds were then allowed to polymerize for 24 h. At the same time, samples of pure epoxy were created in order to provide mechanical comparison. The final composite scaffolds were each cylindrical in shape with an approximate diameter and height of 17 mm and 40 mm respectively. However, in order to avoid the more dense and distorted structures that are known to occur at the bottom of the scaffolds [4,17], ~10 mm was cut off and removed.

## 2.2. Material characterization

The microstructural dimensions of all 24 composite scaffolds were observed with scanning electron microscopy (SEM) at 10 kV and a spot size of 3.0 nm using a Philips XL30 field emission environmental scanning electron microscope (FEI Company, Hillsboro, OR, USA). For SEM preparation, transverse cross-sections were removed from the overall composite scaffolds (the rest of the material was saved for mechanical characterization) and these samples were sputter-coated with iridium using an Emitech K575X sputter coater (Quorum Technologies Ltd., West Sussex, UK). Microstructure measurements of the pore size were performed using ImageJ software (National Institutes of Health, Bethesda, MD, USA). Forty measurements were taken on each sample to calculate the mean and standard deviation. Measurements of pore size and shape were performed by adjusting the threshold of the micrographs (using a consistent threshold for all measurements) so as to fit an ellipse to the pores in order to determine the elliptic major axis,  $a$ , and minor axis,  $b$  (Fig. 2). The assumption of elliptical pores has been previously employed for scaffolds and composite scaffolds with similar architecture [6,18]. From these measurements the pore area,  $A_p$ , and pore aspect ratio  $X_p$ , were calculated as  $A_p = \pi ab / 4$  and  $X_p = a / b$  respectively. In addition, the lamellar wall thickness,  $T_w$ , was measured using the same procedure described above. These microstructural measurements were taken as they are amongst those

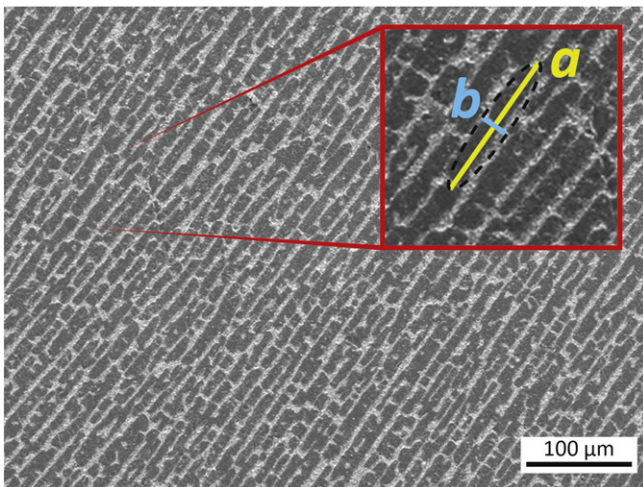


**Fig. 2.** Example micrograph of a two-phase freeze cast bioinspired composite scaffold. Sintered ZrO<sub>2</sub> ceramic is light gray and epoxy polymer is dark gray. Inset highlights an individual pore in order to show the major axis,  $a$ , and minor axis,  $b$ .

most commonly utilized to describe the structure of freeze cast scaffolds in literature [16,18,19].

## 2.3. Volumetric and mechanical characterization

Of the eight prepared composite scaffolds for each set, five were chosen at random for volumetric and mechanical characterization. Each of the five was cut into seven cubic samples of roughly  $5 \times 5 \times 5 \text{ mm}^3$ , as shown in Fig. 1. The ZrO<sub>2</sub> volume percent,  $V_c$ , of these cubic samples was calculated from a rule of mixtures for a two-phase composite:

$$V_c = \frac{\rho_{cs} - \rho_p}{\rho_c - \rho_p} \times 100 \quad (1)$$

where  $\rho_{cs}$ ,  $\rho_p$  and  $\rho_c$  are the final composite scaffold, polymer (Epocure 2) and ceramic (ZrO<sub>2</sub>) densities respectively. The densities  $\rho_{cs}$  and  $\rho_p$  were each calculated by Archimedes' principle. In both cases, the mean of the seven samples was used to determine the final density. This method assumes that the infiltrated composite scaffolds are solely two-phase composites and are devoid of any air pockets, an assumption that was supported by SEM observations of the final composite scaffolds. The polymer density was experimentally calculated while the density of pure ZrO<sub>2</sub> was used,  $\rho_c = 5.89 \text{ g/cm}^3$ .

For each composite scaffold, the seven cubic samples described above were compressed in the ice growth (longitudinal) direction. Compression testing was performed using a 3367 Instron materials testing machine (Instron, Norwood, MA, USA) with a 30 kN static load cell at a constant crosshead velocity of  $0.005 \text{ mm s}^{-1}$ . In addition, samples of the pure infiltrating epoxy were tested using the same condition, by sectioning a sample of epoxy into seven samples of roughly  $5 \times 5 \times 5 \text{ mm}^3$ . The ultimate compressive strength (UCS) and Young's modulus ( $E$ ) were determined from the maximum stress and linear slope of the stress–strain curves respectively.

## 2.4. Statistical analysis

Measurements of  $a$ ,  $b$ ,  $A_p$  and  $X_p$  and the mechanical properties UCS and  $E$  were first analyzed using One-way ANOVA ( $\alpha = 0.05$ ). One-way ANOVA tests (Fig. 3a) determine if the means of all individual composite scaffold measurements with the same solid loading concentration are equal through a comparison of the calculated mean square between composite scaffolds ( $MS_b$ ) and the calculated mean square within an individual composite scaffold ( $MS_w$ ) (e.g. are all of the composite scaffolds producing the same value of  $A_p$ ?). This ratio of the between-groups mean square over within-groups mean square is called the  $F$  statistic [20]:

$$F = \frac{MS_b}{MS_w} \quad (2)$$

From the value of  $F$  and the chosen significance level ( $\alpha = 0.05$  for the tests in this study) a  $p$ -value, which indicates the probability of  $MS_b$  being greater than or equal to  $F \times MS_w$ , was determined. A value of  $F = 1$  would denote that there is no significant difference between composite scaffold measurements. For  $F > 1$ , the greater the value of  $F$ , the more variability exists between composite scaffold measurements compared to within composite scaffold measurements. For example, for measurements of  $A_p$  in all eight composite scaffolds with 15 vol.% ZrO<sub>2</sub> in this study,  $F = 5.939$  and  $p < 0.05$ . This indicates that one or more of the composite scaffolds have values of  $A_p$  that vary significantly from the others.

In addition, post hoc Tukey honest significant difference (HSD) multiple comparison tests (Fig. 3b) were used to investigate significant differences between composite scaffolds with the same solid loading concentration (e.g. is there a statistically significant difference between the measurements of  $A_p$  between two individual samples?). First, a

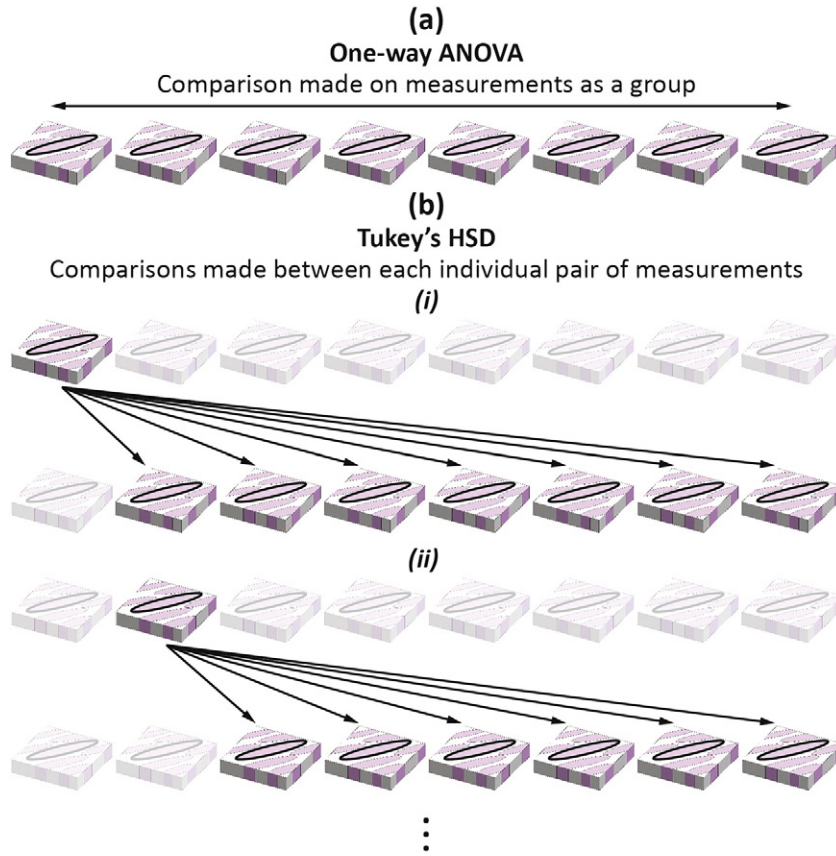


**Fig. 3.** Schematic diagrams of the statistical analyses utilized to determine the statistical significance of the measurements in this study. In all cases, comparisons are made to determine if measurements show no statistically significant differences to  $p < 0.05$  (represented here by arrows). The microstructural measurements of  $a$ ,  $b$ ,  $A_p$ , and  $X_p$  along with the volumetric and mechanical properties of  $V_c$ ,  $E$  and  $UCS$  were all analyzed with this method. (a) One-way ANOVA looks to determine if all measurements are the same amongst a large group of samples but does not distinguish significance between samples; (b) Tukey's HSD determines if two individual, pairwise measurements within the group are the same. Tukey's HSD tests are repeated for every possible pair (e.g. (i), (ii)) of samples.

critical value of the Tukey HSD  $Q$  statistic ( $Q_{crit}$ ) is determined from the Studentized Range distribution ( $\alpha = 0.05$ ). Then, the Tukey HSD test statistic,  $Q_{i,j}$ , is calculated [20]:

$$Q_{i,j} = \frac{|\bar{x}_i - \bar{x}_j|}{(MS_w/n)^{1/2}} \quad (3)$$

where  $\bar{x}_i$  and  $\bar{x}_j$  are the mean measurement values for the two composite scaffolds being compared and  $n$  is the sample size of each measurement group (e.g.  $n = 40$  for microstructural measurements and  $n = 7$  for mechanical property measurements in this study). If  $Q_{i,j} > Q_{crit}$ , there is a statistically significant difference between the composite scaffolds for the given measurement. For example, when comparing measurements of  $A_p$  between these first two composite scaffolds with 15 vol.% ZrO<sub>2</sub> listed in Table 1,  $Q_{i,j} = 3.594$ . This is less than the value of  $Q_{crit} = 4.316$ , therefore there is no significant variance in  $A_p$  between the two samples. These statistical tools have been previously employed to determine the significance of mechanical data in biomedical materials [21,22]; additional information about these methods can be found in Tabachnick and Fidell [20].

### 3. Results and discussion

Microstructural dimensions of the sets of composite scaffolds with 10, 15 and 20 vol.% ZrO<sub>2</sub> are listed in Table 1 and displayed in Fig. 4 (all data points are plotted as mean  $\pm$  one standard deviation). In addition, the global mean values for all composite scaffolds at each solid loading concentration (e.g. values of  $A_p$ , commonly used to describe

**Table 1**

Values of pore major axis,  $a$ , pore minor axis,  $b$ , pore area,  $A_p$ , pore aspect ratio,  $X_p$ , and lamellar wall thickness,  $T_w$ , for all ZrO<sub>2</sub> scaffolds infiltrated with epoxy. Data reported as mean  $\pm$  standard deviation of 40 measurements.

Sample set	$a$ ( $\mu\text{m}$ )	$b$ ( $\mu\text{m}$ )	$A_p$ ( $\mu\text{m}^2$ )	$X_p$	$T_w$ ( $\mu\text{m}$ )
10 vol.% ZrO <sub>2</sub>	71.4 $\pm$ 22.1	18.7 $\pm$ 4.6	1070 $\pm$ 496	3.98 $\pm$ 1.39	4.7 $\pm$ 1.7
	95.8 $\pm$ 31.8	11.9 $\pm$ 2.7	908 $\pm$ 416	8.32 $\pm$ 2.79	3.3 $\pm$ 1.1
	97.1 $\pm$ 34.3	15.5 $\pm$ 4.0	1178 $\pm$ 482	6.74 $\pm$ 3.07	3.3 $\pm$ 1.2
	84.9 $\pm$ 20.7	16.8 $\pm$ 4.4	1132 $\pm$ 386	5.32 $\pm$ 1.91	3.2 $\pm$ 1.4
	84.3 $\pm$ 20.9	16.0 $\pm$ 3.8	1071 $\pm$ 395	5.49 $\pm$ 1.69	3.0 $\pm$ 1.0
	78.1 $\pm$ 21.0	12.4 $\pm$ 2.9	760 $\pm$ 276	6.67 $\pm$ 2.25	2.2 $\pm$ 0.9
	88.0 $\pm$ 28.4	18.9 $\pm$ 4.9	1337 $\pm$ 594	4.91 $\pm$ 1.75	3.3 $\pm$ 1.5
	79.7 $\pm$ 26.1	15.8 $\pm$ 3.7	999 $\pm$ 428	5.31 $\pm$ 2.25	3.0 $\pm$ 0.9
Mean	84.9 $\pm$ 8.7	15.8 $\pm$ 2.6	1057 $\pm$ 175	5.84 $\pm$ 1.34	3.2 $\pm$ 0.7
15 vol.% ZrO <sub>2</sub>	59.6 $\pm$ 26.4	15.4 $\pm$ 3.7	752 $\pm$ 474	3.94 $\pm$ 1.59	6.3 $\pm$ 2.0
	58.0 $\pm$ 25.3	11.9 $\pm$ 3.3	579 $\pm$ 398	4.92 $\pm$ 1.78	4.6 $\pm$ 1.4
	56.0 $\pm$ 27.1	10.8 $\pm$ 2.4	509 $\pm$ 333	5.08 $\pm$ 1.87	5.0 $\pm$ 2.0
	50.1 $\pm$ 16.5	11.4 $\pm$ 2.5	461 $\pm$ 203	4.49 $\pm$ 1.50	4.7 $\pm$ 1.6
	41.4 $\pm$ 20.2	10.1 $\pm$ 2.3	340 $\pm$ 208	4.17 $\pm$ 2.01	5.1 $\pm$ 1.6
	56.5 $\pm$ 19.5	12.5 $\pm$ 2.7	564 $\pm$ 259	4.66 $\pm$ 1.67	5.1 $\pm$ 1.6
	55.6 $\pm$ 19.2	10.9 $\pm$ 2.0	484 $\pm$ 223	5.20 $\pm$ 1.86	4.8 $\pm$ 2.0
	64.5 $\pm$ 24.4	10.8 $\pm$ 1.7	550 $\pm$ 223	6.10 $\pm$ 2.54	4.9 $\pm$ 1.9
Mean	55.2 $\pm$ 6.9	11.7 $\pm$ 1.7	530 $\pm$ 118	4.82 $\pm$ 0.67	5.1 $\pm$ 0.5
20 vol.% ZrO <sub>2</sub>	55.7 $\pm$ 24.1	12.8 $\pm$ 3.3	591 $\pm$ 377	4.41 $\pm$ 1.58	7.5 $\pm$ 3.2
	68.8 $\pm$ 36.0	14.3 $\pm$ 2.7	785 $\pm$ 460	4.87 $\pm$ 2.34	8.1 $\pm$ 2.8
	55.9 $\pm$ 22.6	10.9 $\pm$ 2.6	489 $\pm$ 256	5.26 $\pm$ 2.06	7.5 $\pm$ 1.7
	49.6 $\pm$ 18.7	14.2 $\pm$ 3.1	571 $\pm$ 299	3.54 $\pm$ 1.17	8.3 $\pm$ 2.6
	50.8 $\pm$ 23.7	13.2 $\pm$ 3.1	546 $\pm$ 324	3.90 $\pm$ 1.65	7.1 $\pm$ 2.2
	55.1 $\pm$ 30.3	16.7 $\pm$ 3.2	754 $\pm$ 524	3.28 $\pm$ 1.55	9.2 $\pm$ 3.1
	55.2 $\pm$ 27.1	16.7 $\pm$ 3.2	747 $\pm$ 451	3.34 $\pm$ 1.59	8.8 $\pm$ 3.2
	60.5 $\pm$ 21.0	13.0 $\pm$ 3.3	650 $\pm$ 342	4.69 $\pm$ 1.33	8.1 $\pm$ 3.6
Mean	56.4 $\pm$ 6.0	14.0 $\pm$ 2.0	641 $\pm$ 110	4.16 $\pm$ 0.75	8.1 $\pm$ 0.7

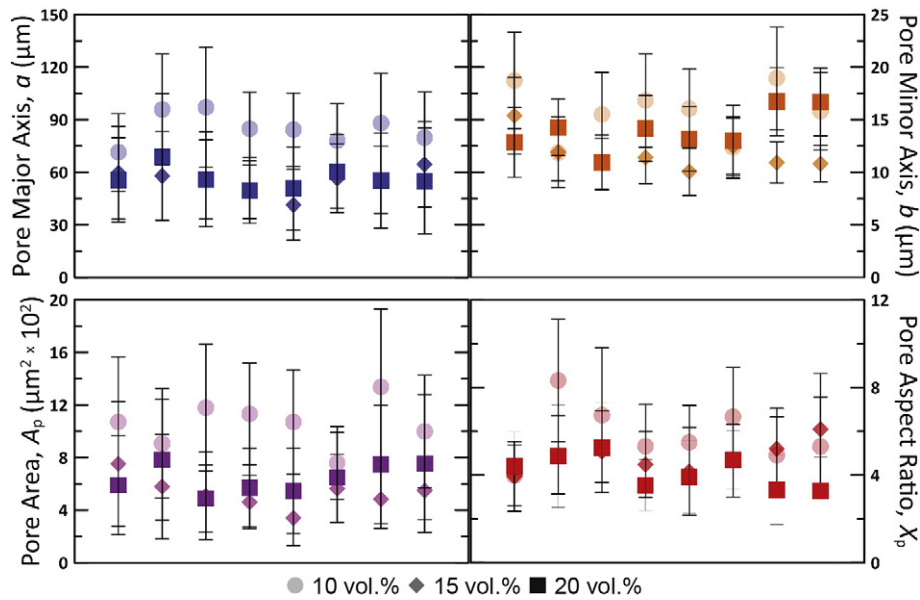


Fig. 4. Microstructural measurements. In each case measurements for each of the eight composite scaffolds are plotted as mean  $\pm$  one standard deviation of 40 measurements.

freeze cast scaffold porosity, = 1057, 530 and 641  $\mu\text{m}^2$  for 10, 15 and 20 vol.%  $\text{ZrO}_2$  respectively) were determined (Table 1). It is of note that the standard deviations are very large, in some cases up to half of the measured mean. All microstructural dimensions for each composite scaffold are roughly within one standard deviation of each other. In addition, the microstructures from each of the sets, as seen in the example micrographs shown in Fig. 5, appear relatively similar. The ANOVA results showed that the microstructural dimensions ( $a$ ,  $b$ ,  $A_p$ ,  $X_p$ ) of each set had significant differences ( $2.1 < F < 17.3$ ,  $p < 0.05$ ), demonstrating that at each solid loading concentration, the composite scaffolds are not similar. This is of note given that, at each solid loading concentration, all eight composite scaffolds were prepared with the exact same processing techniques and conditions and therefore, theoretically, should produce the same microstructure. This suggests that the

processing technique itself is the most likely source of this deviation within the composite scaffolds. This is mostly likely due to the process being dependent upon the growth of ice crystals that template the solid loading and create the pores. As this ice crystal growth is only controlled in a single direction, there is likely a large amount of variability in the exact pattern of the ice growth from sample to sample, thus resulting in the variation in resultant microstructure. Despite the significant potential of the process of freeze casting for biomedical applications, the current results suggest a complication in the mass production of these composite scaffolds for commercialization.

Although the ANOVA analysis showed that the composite scaffolds for each set had statistically significant differences, observing each pair of composite scaffolds in a set through Tukey's HSD test revealed more similarities in many cases (summarized in Table 2).

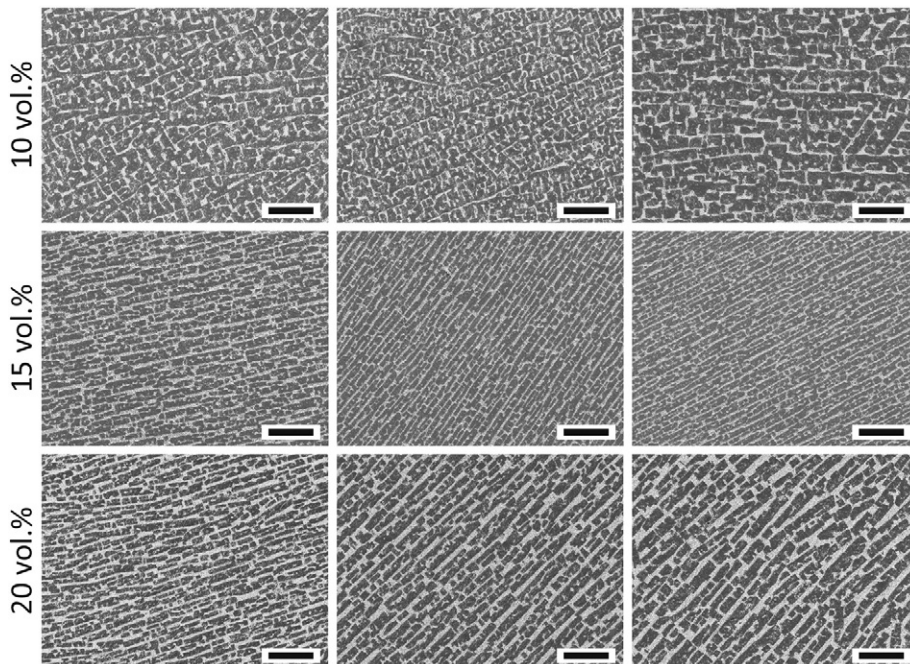


Fig. 5. Three example micrographs for each set of composite scaffolds (10, 15 and 20 vol.%  $\text{ZrO}_2$ ). Microstructures appear relatively similar at each solid loading concentration. Sintered  $\text{ZrO}_2$  ceramic is light gray and epoxy polymer is dark gray. Scale bars: 100  $\mu\text{m}$ .

This test observes the 28 possible pairwise comparisons within each composite scaffold set. Measurements of  $b$  and  $X_p$ , in general, displayed relatively high levels or variability with >50% of pairs showing statistically significant variability in some cases. However, measurements of  $a$  and  $A_p$  at all solid loading concentrations resulted in  $\leq 25\%$  of pairs showing statistically significant variation. The more in-depth Tukey's HSD test highlights that the majority of microstructures were similar within the measurements of  $a$  and  $A_p$ . This enforces the importance of performing this post-hoc test in order to better understand the statistical significance of results as, for some applications, specific measurements (such as  $A_p$  in cases where infiltration is important) may be of greater priority.

Previous research has shown that changes in the microstructural measurements analyzed here can greatly alter the mechanical properties [6,7,18].  $E$ ,  $UCS$  and  $V_c$  are listed in Table 3 and  $E$  and  $UCS$  are displayed in Fig. 6 for all five composite scaffolds at each solid loading concentration. When compared to the experimentally determined properties of the infiltrating epoxy, the mean composite scaffold was able to provide at least modest gains. Each composite scaffold only consists of ~15–27 vol.% ZrO<sub>2</sub>; however, the mechanical properties are considerably lower than what would be expected by a simple rule of mixtures, which predicts  $UCS \approx 400$ – $650$  MPa (using values of infiltrating epoxy and ZrO<sub>2</sub> monoliths from Table 3), which is considerably larger than the measured values of  $UCS \approx 105$ – $125$  MPa. This is likely due to internal porosity within the lamellar walls, which has been previously reported to have a significant effect upon the mechanical properties of freeze cast scaffolds [18]. This would also explain the low values for  $E$ , as the porous walls would be unable to provide their ideal (dense) elastic strength. This could be improved by altering the sintering conditions, such as increasing the temperature or adding a sintering aid, both of which would increase the density of the lamellar walls.

When observed visually in Fig. 6, mechanical properties within each solid loading are generally always within one standard deviation of each other. However, ANOVA analysis showed that the measurements of  $E$  and  $UCS$  for composite scaffold sets, regardless of solid loading concentration, had significant differences ( $3.1 < F < 8.3$ ,  $p < 0.05$ ), with the exception of values of  $E$  for 20 vol.% ZrO<sub>2</sub>. However, as observed for the microstructures, Tukey's HSD tests revealed that relatively few of the 10 possible pairwise comparisons, only 20% and 30% of pairs for  $E$  in scaffold composites with 10 and 15 vol.% ZrO<sub>2</sub>, respectively and 20%, 20% and 40% of pairs for  $UCS$  in scaffold composites with 10, 15 and 20 vol.% ZrO<sub>2</sub>, respectively, showed statistically significant differences (Table 2). While these results support previous reports that changes in the microstructure can be connected to variability in the mechanical properties, the majority of composite scaffolds were able to produce comparable mechanical properties or, as was the case for the moduli of scaffolds with 20 vol.% ZrO<sub>2</sub>, mechanical properties that showed no statistical differences.

It is the explicit intent of this work to observe the reproducibility of ZrO<sub>2</sub>-based freeze casting with a consistent set of processing parameters. However, as the three composite scaffold sets within this work vary through only one parameter (the solid loading concentration) it

**Table 2**

Summary of results from the Tukey HSD tests. Results are presented as the % of significant different pairwise comparisons for microstructural measurements (28 pairs) and mechanical properties (10 pairs).

Sample set	Microstructural (%)				Mechanical properties (%)	
	$a$	$b$	$A_p$	$X_p$	$UCS$	$E$
10 vol.% ZrO <sub>2</sub>	11	61	25	67	20	20
15 vol.% ZrO <sub>2</sub>	11	32	25	14	20	30
20 vol.% ZrO <sub>2</sub>	7	54	4	32	40	N/A <sup>a</sup>

<sup>a</sup> ANOVA found no statistically significant differences in values of  $E$  between scaffolds with 20 vol.% ZrO<sub>2</sub>. Therefore no Tukey HSD test was necessary.

**Table 3**

Values of ultimate compressive strength,  $UCS$ , Young's modulus,  $E$ , and ceramic volume percent,  $V_c$ , for all samples. In addition, experimentally determined mechanical properties for the infiltrating epoxy are included. Data reported as mean  $\pm$  standard deviation of seven measurements.

Sample set	$UCS$ (MPa)	$E$ (GPa)	$V_c$ (vol.% ZrO <sub>2</sub> )
10 vol.% ZrO <sub>2</sub>	103.5 $\pm$ 16.7	2.59 $\pm$ 0.58	13.8 $\pm$ 1.1
	112.5 $\pm$ 15.0	3.17 $\pm$ 0.67	13.6 $\pm$ 1.2
	107.9 $\pm$ 7.5	2.66 $\pm$ 0.39	12.7 $\pm$ 0.5
	92.9 $\pm$ 12.6	1.93 $\pm$ 0.39	14.5 $\pm$ 1.3
	113.7 $\pm$ 8.9	2.68 $\pm$ 0.16	15.8 $\pm$ 0.4
Mean	106.1 $\pm$ 14.1	2.61 $\pm$ 0.60	14.1 $\pm$ 1.4
15 vol.% ZrO <sub>2</sub>	150.6 $\pm$ 25.8	4.25 $\pm$ 1.02	27.1 $\pm$ 0.4
	107.5 $\pm$ 42.4	1.80 $\pm$ 1.03	26.2 $\pm$ 1.7
	130.6 $\pm$ 17.1	2.40 $\pm$ 0.97	28.2 $\pm$ 0.5
	136.0 $\pm$ 20.0	3.16 $\pm$ 0.80	24.1 $\pm$ 1.1
	99.7 $\pm$ 26.1	2.60 $\pm$ 0.88	28.4 $\pm$ 1.6
Mean	124.9 $\pm$ 32.2	2.84 $\pm$ 1.22	26.8 $\pm$ 1.9
20 vol.% ZrO <sub>2</sub>	140.7 $\pm$ 17.9	2.98 $\pm$ 0.70	27.4 $\pm$ 0.7
	134.8 $\pm$ 21.6	3.26 $\pm$ 0.74	27.2 $\pm$ 0.6
	124.3 $\pm$ 10.8	2.12 $\pm$ 0.43	28.8 $\pm$ 0.7
	92.3 $\pm$ 14.5	2.70 $\pm$ 0.81	23.0 $\pm$ 1.0
	133.5 $\pm$ 21.3	3.12 $\pm$ 1.05	28.0 $\pm$ 1.8
Mean	125.1 $\pm$ 24.1	2.84 $\pm$ 0.83	26.9 $\pm$ 2.3
Infiltrating epoxy	79.9 $\pm$ 4.0	1.80 $\pm$ 0.35	
ZrO <sub>2</sub> monoliths [29,30]	2200 $\pm$ 522	205 $\pm$ 5	

can also be noted that this processing method may not be able to consistently produce variation of the mechanical properties. Previous results on freeze cast scaffolds show an increasing trend in pore size with decreasing initial solid loading concentration [16,23]. However, there is known to be significant scatter in data linking initial solid loading concentration to final pore size due to numerous effects during freeze casting such as the size distribution and morphology of the particles [16,23]. Regardless, it would be logical to suggest that composite scaffolds with more solid loading would produce higher mechanical properties. This is seen when observing the difference between 10 and 15 vol.%, however, as can be seen in Fig. 6 as well as Table 3, the mean mechanical properties and  $V_c$  between scaffold composites with 15 and 20 vol.% ZrO<sub>2</sub> are effectively the same. The only parameter to vary consistently is  $T_w$ , which increases with increased solid loading concentration (Table 1). It has been previously reported in freeze cast scaffolds with hydroxyapatite that increasing the solid loading concentration makes it more difficult for a freezing front moving through the slurry to repel the solid particles [16], which would lower the freezing front velocity,  $\nu$ . The freezing front dendritic ice wavelength,  $\lambda = b + T_w$  is proportional to  $1/\nu$ . The current data shows that the mean  $\lambda$  increases from 16.8 to 22.1  $\mu\text{m}$  between 15 and 20 vol.% (Table 1). A decrease in  $\nu$  due to higher solid loading increases  $\lambda$ , which results in the enlarged pores observed for 20 vol.% ZrO<sub>2</sub>. This is proposed to be the cause of the relatively similar mechanical results between 15 and 20 vol.% ZrO<sub>2</sub>. When considering  $V_c$ , it is well known that there is a structural gradient within freeze cast scaffolds with more dense material (which would hold a higher concentration of solid loading particles) at the initial ice nucleation front giving way to lamellar ice growth (associated with the lamellar wall microstructures observed here) further through the scaffold [24]. In order to avoid this dense structure, all samples for microstructural and mechanical testing have been taken far from the surface where the ice originally nucleated. However, it has been reported that a slower  $\nu$  (as is proposed to be present in 20 vol.% ZrO<sub>2</sub>) results in a smaller structural gradient throughout the scaffold [24], which would result in a relatively larger volume of dense material near the initial ice nucleation front. This would result in a lower proportion of solid loading within the observed lamellar region of the scaffolds and is proposed to be the cause of the lower than expected  $V_c$  results at 20 vol.% ZrO<sub>2</sub>. However, to the

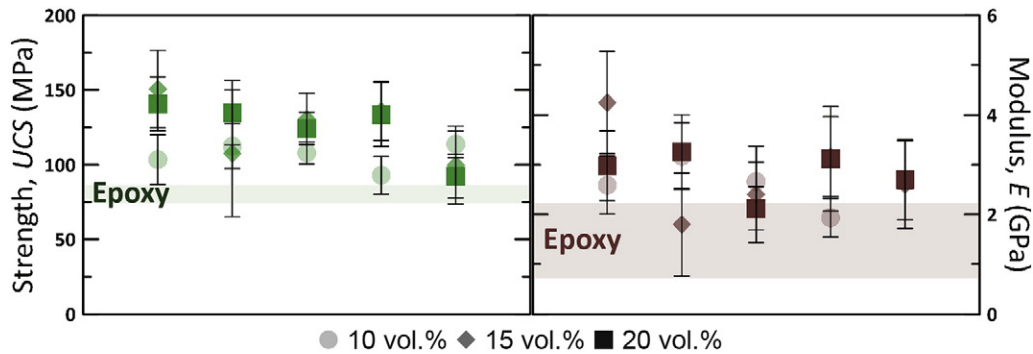


**Fig. 6.** Mechanical properties. In each case measurements for each of the five composite scaffolds are plotted as mean  $\pm$  one standard deviation of seven measurements. Bands are shown that represent the mean  $\pm$  one standard deviation of experimentally determined mechanical properties for the infiltrating epoxy.

knowledge of the authors, there are no kinetic models for the growth of ice interacting with solid particles that take into account the concentration of particles. This highlights an area of research into freeze casting that must be further investigated in order to improve the reproducibility of the process.

The current results prove the variability of the freeze casting process. Of note individual pairings (i.e. individual values of  $UCS$  for samples of 15 and 20 vol.%  $ZrO_2$ ) of the samples show the expected trends (e.g. decreased  $A_p$ , increased  $UCS$  with increasing solid loading concentration). However, the variability between composite scaffolds results in pairings that show the opposite trends as well.

The process of freeze casting holds significant potential for biomedical and structural applications, but the current results highlight that reproducibility of scaffolds and composite scaffolds will likely stand as an impediment to mass-production or commercialization. However, while predominantly not statistically reproducible, the microstructures and properties created through the freeze casting process in this study did show a great deal of similarity (as determined through Tukey's HSD tests). This provides hope that additional research and refinement of the freeze casting method may be able to provide reproducible materials. There are a number of simple alterations to the process that could improve the reproducibility. To ensure homogeneity between slurries they could be produced in a single batch as opposed to individually. During freezing, heterogeneous ice nucleation can be reduced by controlling the temperature to provide a more uniform freezing front, using a larger mold to avoid edge effects and smoothing the mold walls. In addition, one of the largest contributors is likely to be that the process is generally only controlled in a single direction. As the slurry is directionally frozen in the principal step of freeze casting, the direction of ice growth is the only true control of the process. The recent example of magnetic freeze casting [25–27] provides control of the microstructure in multiple orthogonal directions through both the ice crystal growth and an applied magnetic field (oriented perpendicular to the ice growth during the freezing process). Additionally, scaffolds with a centrosymmetric structure have been reported that employ two cold sources oriented at perpendicular directions, thus inducing two ice growth directions [28]. Additional research into methods such as these that provide control in multiple directions may provide more reproducible microstructures and properties.

#### 4. Conclusions

The current experimental study of the reproducibility of epoxy-infiltrated, freeze cast  $ZrO_2$  composite scaffolds enables the following conclusions:

- Based upon a One-way ANOVA test, statistically significant variability between scaffolds was determined in all microstructural dimensions regardless of the solid loading concentration ( $a$ ,  $b$ ,  $A_p$  and  $X_p$ ). As a result, the scaffolds within this study cannot be said to be the same.

Post-processing through Tukey's HSD tests revealed that, regardless of solid loading concentration, the majority of scaffolds produced similar measurements of  $a$  and  $A_p$ , as  $\leq 25\%$  of pairs showed statistically significant variability.

- Mechanical properties (Young's modulus,  $E$ , and ultimate compressive strength,  $UCS$ ) showed statistically significant variability between samples in almost all cases in a One-way ANOVA test. The sole exception came when observing scaffold composites with 20 vol.%  $ZrO_2$  where no significant differences were found within values for  $E$  between scaffold samples. Post-processing through Tukey's HSD tests revealed that in all cases, the majority of pairs for  $E$  and  $UCS$  showed no statistically significant variability.
- While not similar overall, results from Tukey's HSD tests revealed that many of the composite scaffolds fabricated in this study were similar in specific microstructural and mechanical properties.
- Freeze casting holds significant potential for biomedical applications, but more research is required in order to ensure reliable production of similar scaffold microstructures and mechanical properties.

#### Acknowledgments

This work is supported by a Multi-University Research Initiative through the Air Force Office of Scientific Research of the United States (AFOSR-FA9550-15-1-0009). The authors wish to acknowledge Dr. Antoni Tomsia for generously introducing us to the freeze casting process and Michael B. Frank, Christopher F. Yu, Rachel Hsiong and Michael Ix for their help with the freeze casting process.

#### References

- [1] E. Munch, M.E. Launey, D.H. Alsem, E. Saiz, A.P. Tomsia, R.O. Ritchie, Tough, bio-inspired hybrid materials, *Science* 322 (2008) 1516–1520.
- [2] E. Munch, E. Saiz, A.P. Tomsia, S. Deville, Architectural control of freeze-cast ceramics through additives and templating, *J. Am. Ceram. Soc.* 92 (2009) 1534–1539.
- [3] S. Deville, E. Saiz, R.K. Nalla, A.P. Tomsia, Freezing as a path to build complex composites, *Science* 311 (2006) 515–518.
- [4] S. Deville, E. Saiz, A.P. Tomsia, Ice-templated porous alumina structures, *Acta Mater.* 55 (2007) 1965–1974.
- [5] M.M. Porter, J. McKittrick, M.A. Meyers, Biomimetic materials by freeze casting, *JOM* 65 (2013) 720–727.
- [6] S.E. Naleway, C.F. Yu, M.M. Porter, A. Sengupta, P.M. Iovine, M.A. Meyers, J. McKittrick, Bioinspired composites from freeze casting using clathrate hydrates, *Mater. Des.* 71 (2015) 62–67.
- [7] M.M. Porter, M. Yeh, J. Strawson, T. Goehring, S. Lujan, P. Siripapaporn, M.A. Meyers, J. McKittrick, Magnetic freeze casting inspired by nature, *Mater. Sci. Eng. A* 556 (2012) 741–750.
- [8] S. Deville, Ice-templating, freeze casting: beyond materials processing, *J. Mater. Res.* 28 (2013) 2202–2219.
- [9] F. Bouville, E. Maire, S. Meille, B. VAN DE Moortele, A.J. Stevenson, S. Deville, Strong, tough and stiff bioinspired ceramics from brittle constituents, *Nat. Mater.* 13 (2014) 508–514.
- [10] J. Binner, H. Chang, R. Higginson, Processing of ceramic–metal interpenetrating composites, *J. Eur. Ceram. Soc.* 29 (2009) 837–842.

- [11] H.M. Chen, Y.F. Yin, H.B. Dong, Y. Tong, M. Luo, X. Li, Porous alumina infiltrated with melt and its dynamic analysis during pressureless infiltration, *Ceram. Int.* 40 (2014) 6293–6299.
- [12] B.S. Rao, V. Jayaram, New technique for pressureless infiltration of Al alloys into  $Al_2O_3$  preforms, *J. Mater. Res.* 16 (2001) 2906–2913.
- [13] U.G.K. Wegst, H. Bai, E. Saiz, A.P. Tomsia, R.O. Ritchie, Bioinspired structural materials, *Nat. Mater.* 14 (2015) 23–36.
- [14] U.G.K. Wegst, M. Schechter, A.E. Donius, P.M. Hunger, Biomaterials by freeze casting, *Phil. Trans. R. Soc. A* 368 (2010) 2099–2121.
- [15] Z.M. Xia, X.H. Yu, X. Jiang, H.D. Brody, D.W. Rowe, M. Wei, Fabrication and characterization of biomimetic collagen–apatite scaffolds with tunable structures for bone tissue engineering, *Acta Biomater.* 9 (2013) 7308–7319.
- [16] S. Deville, E. Saiz, A.P. Tomsia, Freeze casting of hydroxyapatite scaffolds for bone tissue engineering, *Biomaterials* 27 (2006) 5480–5489.
- [17] S. Deville, E. Maire, A. Lasalle, A. Bogner, C. Gauthier, J. Leloup, C. Guizard, In situ X-ray radiography and tomography observations of the solidification of aqueous alumina particle suspensions – part I: initial instants, *J. Am. Ceram. Soc.* 92 (2009) 2489–2496.
- [18] M.M. Porter, R. Imperio, M. Wen, M.A. Meyers, J. McKittrick, Bioinspired scaffolds with varying pore architectures and mechanical properties, *Adv. Funct. Mater.* 24 (2013) 1978–1987.
- [19] S. Deville, Freeze-casting of porous ceramics: a review of current achievements and issues, *Adv. Eng. Mater.* 10 (2008) 155–169.
- [20] B.G. Tabachnick, L.S. Fidell, *Using Multivariate Statistics*, 6 ed. Boston, MA, Pearson, 2013.
- [21] J. Manhart, K.H. Kunzelmann, H.Y. Chen, R. Hicckel, Mechanical properties of new composite restorative materials, *J. Biomed. Mater. Res.* 53 (2000) 353–361.
- [22] M. Albakry, M. Guazzato, M.V. Swain, Fracture toughness and hardness evaluation of three pressable all-ceramic dental materials, *J. Dent.* 31 (2003) 181–188.
- [23] S. Deville, Freeze-casting of porous biomaterials: structure, properties and opportunities, *Materials* 3 (2010) 1913–1927.
- [24] S. Deville, E. Maire, A. Lasalle, A. Bogner, C. Gauthier, J. Leloup, C. Guizard, Influence of particle size on ice nucleation and growth during the ice-templating process, *J. Am. Ceram. Soc.* 93 (2010) 2507–2510.
- [25] M.M. Porter, *Bioinspired Design: Magnetic Freeze Casting* (Ph.D. thesis), University of California, San Diego, 2014.
- [26] M.M. Porter, L. Meraz, A. Calderon, H. Choi, A. Chouhan, L. Wang, M.A. Meyers, J. McKittrick, Torsional properties of helix-reinforced composites fabricated by magnetic freeze casting, *Compos. Struct.* 119 (2015) 174–184.
- [27] M.M. Porter, J. McKittrick, It's tough to be strong: advances in bioinspired structural ceramic-based materials, *Am. Ceram. Soc. Bull.* 93 (2014) 18–24.
- [28] Y.F. Tang, Q. Miao, S. Qiu, K. Zhao, L. Hu, Novel freeze-casting fabrication of aligned lamellar porous alumina with a centrosymmetric structure, *J. Eur. Ceram. Soc.* 34 (2014) 4077–4082.
- [29] C. Piconi, G. Maccauro, Zirconia as a ceramic biomaterial, *Biomaterials* 20 (1999) 1–25.
- [30] K.J. Chun, J.Y. Lee, Comparative study of mechanical properties of dental restorative materials and dental hard tissues in compressive loads, *J. Dent. Biomech.* 5 (2014) 1–6.